SMC with Disturbance Observer for a Linear Belt-Drive

Aleš Hace, *Member, IEEE*, Karel Jezernik, *Senior Member, IEEE*, Asif Šabanović, *Senior Member, IEEE*

Abstract

Accurate position tracking control in a belt-driven servomechanism can experience vibrations and large tracking errors due to compliance and elasticity introduced by force transmission through the belt and nonlinear friction phenomenon. In this paper, a new control algorithm based on sliding mode control that is able to deal with these problems is proposed. In order to further optimize position tracking performance the control scheme has been extended by an asymptotic disturbance observer. It has been proven that robust and vibration-free operation of a linear belt-driven system can be achieved. The experiments presented in the paper show improved position tracking error response while maintaining vibration suppression.

Keywords

motion control, sliding mode control, disturbance observer, timing-belt drive, vibration suppression

Corresponding author:

Dr. Aleš Hace
Faculty of Electrical Engineering and Computer Science
University of Maribor
Smetanova ulica 17, SI-2000 Maribor, Slovenia
phone: +386 2 2207307
fax: +386 2 2207315
email: ales.hace@uni-mb.si

Aleš Hace and Karel Jezernik are with the Institute of Robotics, Faculty of Electrical Engineering and Computer Science, University of Maribor, Slovenia (e-mail: ales.hace@uni-mb.si, karel.jezernik@uni-mb.si). Asif Šabanović is with Faculty of Engineering and Natural Sciences, Sabanci University, Istanbul, Turkey (email: asif@sabanciuniv.edu.tr).

This paper has been previously published in a shorter form in Proceedings of IEEE ISIE'05, June 20-23, 2005, Dubrovnik, Croatia, pp. 1641-1646.

I. INTRODUCTION

Modern mechatronic products such as laser- or waterjet- cutting machines often require servodrives' operation at high speed and high accuracy. However, a frequency dependent characteristic of force transmission in a drive train prevents to achieve required performance. Moreover, control effort aiming to achieve rapid response and accurate position tracking causes vibrations in the mechanical drive system due to undesired resonance frequencies. Thus, a control algorithm has to be designed so to ensure wider frequency bandwidth of the position servo system while it has to be robust against parameters variations and unmodeled dynamics.

The use of timing belts in drive trains is attractive due to their characteristics allowing high speed operation, high efficiency, long travel length and low-cost. On the other hand, drives with timing-belt transmission yield higher transmission error since they feature elasticity, compliance and often more friction than more rigid screw ball drives thus having lower repeatability and accuracy [1]. Consequently, position sensor in a linear belt drive may be often mounted on the load-side. In such setup an application of conventional control like PI, PD or PID approach often fails since belt drives introduce more resonance frequencies [2], which can cause vibrations if not properly suppressed. Such typical response is depicted by Fig.1. In order to attain high performance an advanced control strategy has to be developed. Hori [3] has given a review of advanced methods that deal with torsional vibrations. Various methods have been applied that use acceleration feedback [4][5] or joint torque feedback [6][7]. Furthermore, the well-known disturbance observer approach [6] has been also investigated in the problem of vibration suppression. It turns in “resonance ratio control” [8][9]. One of the important conclusions is that in order to succeed in the vibration controller design the resonance ratio of “anti-resonant frequency” and “resonant frequency” of the system should be considered. It has been shown that development of a general method that can be applicable to a wide variation resonance ratio is complicated. The problem is related to the dynamics of the resonance ratio estimation. The estimation of the resonance ratio plays an important role in the application of this method.

Although the research of a flexible joint or elastic link control is widely present in the robotics related works, only few reports address the load side disturbance compensation and position control problem [10][11], which is a key issue in position tracking of linear belt-driven servodrives. High performance of a linear belt-driven servomechanism requires that the plant parameter variations, uncertain dynamics, and disturbances have to be compensated to guarantee accurate vibration free positioning. Robust system behavior is a prerequisite to achieve this goal. As some authors already reported [10][13][14], one can apply Sliding Mode Control (SMC) [15] to achieve robustness of a belt-driven servosystem. The SMC approach guarantees robustness to model perturbation, parameter variations and exogenous disturbances. However, it requires discontinuous control action that will ensure the ideal performance. In motion control, it can cause well-known chattering and ultimately damage the drive train. Consequently, chattering-free SMC implementation with continuous control action is required [16]. Hace [17] and later Šabanovič [18] have shown that vibration-free performance can be achieved by introduction of belt-stretch control. In [17] the authors have proposed the position tracking control law that has involved the inner-loop with PD belt-stretch controller for vibration suppression and robust position control scheme in the outer-loop (Fig.2-a). Although such engineering approach has been successfully applied in the industrial application [19], practice has shown that it suffers from “trial-and-error” parameter tuning method. Thus, the authors in [20] have presented a new, single-loop SMC algorithm with vibration suppression capability (Fig.2-b). The proposed method introduced improved parameter tuning approach, and furthermore extended closed-loop bandwidth. However, position tracking error peaks still appear at the points of velocity reversals due to nonlinear stiction and friction phenomenon.

Chattering free implementation of SMC impairs the ideal robust behavior of a closed-loop system. The authors in [21] has combined SMC with linear robust control in order to achieve robust servo system. The undesired bang-bang control action still remain in the design, however, recently, a combination of chattering-free SMC design and disturbance observer has been proposed in order to improve performance of a closed-loop system [21]. Following this idea, in this paper, a new SMC control algorithm combined

with an asymptotic disturbance observer for a linear belt-driven servomechanism is proposed (Fig.2-c). The proposed algorithm has been experimentally investigated. It has been proven by experiments that it furthermore improve closed-loop performance of a linear belt-drive.

The paper is organized as follows: the model of a linear belt-drive is developed in the 2nd section, the 3rd section presents derivation of the proposed algorithm, experimental results are shown in the 4th section, which follows with conclusions in the 5th section.

II. MATHEMATICAL MODEL

A typical linear belt-drive is presented in Fig.3-a. It consists of a motor, a speed reducing gear and a belt. The belt drive converts rotation of the motor into linear motion of the carriage. The carriage, whose position is to be controlled, represents the load side of the system.

A. Three-mass model

The belt-drive as depicted by Fig.3-b consists of a timing belt, a carriage and two pulleys: a driving pulley and a driven pulley that stretch the belt, which transmits force from the driving pulley to the carriage. It represents a complex non-linear distributed parameter system. The mathematical model of the belt-driven servomechanism can be obtained using modal analysis. Detailed development of the model can be found in [18]. Under assumptions that (a) the motor can ensure a high-dynamic torque response with a negligible time delay, (b) link between motor shaft and the driving pulley is rigid, (c) no backlash is present in the system, (d) the belt can be modeled by linear mass-less spring, (e) friction that is concentrated in the motor and pulley bearings, the speed reducer (gearbox), and in the carriage guidance, are considered as an unknown exogenous disturbance, one can develop the sixth order mathematical model that is presented by the motion equations (1),

$$\begin{aligned} \left(J_1 + G^2(J_G + J_m)\right)\cdot\ddot{q}_1 + \tau_{f1} &= G\tau - R\cdot\left[K_1(x)\cdot\left(Rq_1 - x\right) - K_3\cdot\left(Rq_2 - Rq_1\right)\right] \\ J_2\ddot{q}_2 + \tau_{f2} &= R\cdot\left[K_2(x)\cdot\left(x - Rq_2\right) - K_3\cdot\left(Rq_2 - Rq_1\right)\right] \\ M_c\ddot{x} + f_f &= K_1(x)\cdot\left(Rq_1 - x\right) - K_2(x)\cdot\left(x - Rq_2\right) \end{aligned} \tag{1}$$

where:

- J_1, J_2: inertia moment of the driving and the driven pulley, respectively,
- J_G, J_m: inertia moment of the speed reducer and the motor, respectively,
- M_c : mass of the carriage,
- G: speed reducer ratio,
- R: radius of the pulleys,
- K_1, K_2, K_3: position dependant elasticity coefficients of the belt,
- q_1, q_2, φ: angular position of the driving pulley, driven pulley, and the motor, respectively,
- x: carriage position,
- τ: torque developed by the motor,
- τ_{f1}, τ_{f2}: friction torque which affects the pulleys,
- f_f: friction force on the carriage.

B. Two-mass model

The model (1) is a highly-coupled and nonlinear system with exogenous disturbances which enter at the driving side as well as the load side of the system. However, the pulley inertia is small in comparison with the motor and the load side inertia. Therefore, the model can be simplified and reduced to a two-mass system. One can obtain the 4th order linear model with constant parameters (2),

$$\begin{aligned} J\ddot{\varphi} + \tau_f &= \tau - \tau^{reac} \\ M\ddot{x} + f_f &= f^{reac} \end{aligned} \tag{2}$$

where J and M denote the motor inertia and the load mass, respectively, τ_f and f_f stands for friction that perturb the system (2). $\tau^{reac} = Lf^{reac}$, $f^{reac} = Kw$, $w = L\varphi - x$ denote reaction torque and force, and belt-stretch, respectively. K is the elasticity coefficient of the belt, and $L = R/G$ is the transmission constant of the linear belt-drive.

C. Two-mass belt-stretch model

The mathematical model (2) can be further rearranged according to the vibration analysis of belt-drives [2]. One can express dynamics of the belt stretch w. If one assume unit transmission constant ($L=1$) to simplify further algebra, then (2) can be rewritten as in (3),

$$\begin{aligned} J\ddot{w} + K_w w &= \tau - \tau_{wf} \\ M\ddot{x} + f_f &= Kw \end{aligned} \tag{3}$$

where $\tau_{wf} = \tau_f - \kappa f_f$, $K_w = K(1+\kappa)$. $\kappa = J/M$ stands for so called inertia ratio. Typical characteristics of an elastic system is the resonant frequency given by (4).

$$\omega_0 = \sqrt{\frac{K}{J}(1+\kappa)} \tag{4}$$

The block scheme of the linear belt-driven servomechanism model that will be employed in the control design is depicted by Fig.4.

III. CONTROL DESIGN

A. Chattering-free Sliding Mode Control Approach

For systems with bounded control input SMC can be used if the uncertainties in the model structure are bounded [15] and full disturbance rejection is possible if so-called matching condition [23] is fulfilled. The system (3) can be described in the following form

$$\begin{aligned} \dot{z}_i &= z_{i+1} \\ \dot{z}_n &= f(\mathbf{z}) + b(\mathbf{z})u + d(t) \end{aligned}$$

where $i = 1,...,n-1$, $\mathbf{z}^T = [z_1,...,z_n]$ is a system state vector, u is scalar input, and $f(\mathbf{z})$, $b(\mathbf{z})$ are nonlinear functions of the system state vector. In the SMC approach, the goal of control design is to find such control input u that restricts the motion of the system states $\mathbf{z}$ to a selected sliding manifold $\sigma(\mathbf{z},t)=0$. This motion is called sliding mode and convergence of the system states to the sliding manifold is referred to as reaching phase. $\sigma(\mathbf{z},t)$ is switching function that can be often selected as a linear

combination of system states and time-variant reference, i.e. $\sigma(\mathbf{z},t) = r(t) - \mathbf{Gz}$. It has been proven that control with discontinuities on the sliding manifold $\sigma(\mathbf{z},t) = 0$ such as

$$u = \begin{cases} u^+, & \sigma(\mathbf{z},t) > 0 \\ u^-, & \sigma(\mathbf{z},t) < 0 \end{cases}$$

can enforce sliding mode if u^+ and u^- are selected such that the derivative of Lyapunov function candidate $v = \sigma^2 / 2$ is negative definite. Since in our case $f(\mathbf{z})$ and $d(t)$ satisfy matching conditions, dynamics of the closed loop system in sliding mode are fully rejecting these disturbances. The SMC control reduces order of the closed loop system. However, the discontinuous control has disadvantages related to the bang-bang control action. Such discontinues control must be strictly avoided in mechanical systems, since it causes well known chattering that may lead to increased wear of the actuators and to excitation of the high order unmodeled dynamics what can cause damage on mechanical parts of the servo system.

Another solution can be found by augmenting the original system with an additional system state in order to eliminate discontinuities on the control signal. It yields

$$\dot{z}_i = z_{i+1}$$
$$\dot{z}_{n+1} = g(\mathbf{z},u) + b(\mathbf{z})\dot{u} + \dot{d}(t)$$

where $g(\mathbf{z},u) = \dot{f}(\mathbf{z}) + \dot{b}(\mathbf{z})u$, $i = 1,...,n$. The derivative of v may have form $\dot{v} = -D\sigma^2$, $D > 0$ [16]. From condition $\sigma\dot{\sigma} = -D\sigma^2$ and by application of the equivalent control method [15] one can derive control u

$$u = \int_0^t \dot{u} d\upsilon$$
$$\dot{u} = \dot{u}_{eq} + D\sigma$$

that assures invariant system motion in sliding mode. The equivalent control $\dot{u}_{eq}$ is solution of $\dot{\sigma}\big|_{\sigma=0} = 0$.

B. Derivation of Control Law

The chattering-free SMC design presented in previous section suggests the use of a switching function of second order in motion control, e.g. $\sigma_2 = r(t) - (\ddot{x} + K_v\dot{x} + K_p x)$. However, as proposed in [20], the sliding mode manifold for the elastic system (3), can be constructed by the following switching function:

$$\sigma = r(t) - \left[\ddot{x} + K_v \dot{x} + K_p x + \gamma(\ddot{w} + \alpha \dot{w}) \right] \tag{5}$$

where K_v, K_p, α, and γ are arbitrary chosen positive control gains. The extended switching function (5) involves also non-rigid modes of the elastic servo system by introducing belt-stretch motion. It is selected in order to achieve asymptotically stable motion dynamics in sliding mode and to cope with the first resonance frequency ω_0. Indeed, by consideration of the model (3) and the switching function definition (5), where the signals $\dot{w}$ and $\ddot{w}$ are replaced by the first and second derivative of the expression

$$w = \tfrac{M}{K} \ddot{x} + \tfrac{1}{K} f_f, \tag{6}$$

respectively, one can derive (7),

$$\beta r(t) - \left[\dddot{x} + \alpha \ddot{x} + \beta \ddot{x} + \beta K_v \dot{x} + \beta K_p x \right] = \beta \sigma + \left(\ddot{f}_f + \alpha \dot{f}_f \right) / M \tag{7}$$

where $\beta = \gamma^{-1} K / M > 0$. The right-hand side of (7) involves not only the switching function signal σ, which should disappear in sliding mode, but also another component, i.e. friction of the load-side f_f, or more precisely, its first and second derivative. This component should not be involved in case of robust sliding mode control, however, the load-side friction can not be considered as matched disturbance signal [23]. Therefore, the system motion in sliding mode can not be decoupled from this signal. Nevertheless, in our case, it will be compensated in steady state.

However, if one choose $r(t) = K_p x_r(t)$ then it is easy to show that the system motion dynamics on the sliding manifold (5) will be specified by the following transfer function:

$$\frac{x(p)}{x_r(p)} = \frac{\beta K_p}{p^4 + \alpha p^3 + \beta p^2 + \beta K_v p + \beta K_p} \tag{8}$$

The parameters of the transfer function (8) can be selected arbitrary in order to prescribe the dynamics of the position closed-loop (the control gain γ from (5) must be calculated as $\gamma = \beta^{-1} K / M$). In sliding mode, the belt-stretch dynamics, which determines vibrations in the drive response, will be characterized by the transfer function (9),

$$H_w(p) = \frac{\beta}{p^2 + \alpha p + \beta} \tag{9}$$

where $\sqrt{\beta}$ determines the natural frequency of the closed-loop. One can notice that by adoption of the transfer function (9) the dynamics (7) can be described by the following form

$$p^2 x = H_w(p)\left(a^c - \sigma\right) + \left(1 - H_w(p)\right) f_f / M \,, \tag{10}$$

where

$$a^c = r(t) - \left(K_v \dot{x} + K_p x\right). \tag{11}$$

The desired dynamics (8) of our closed-loop system that is to be enforced in the ideal sliding mode, that is decoupled from every disturbance signal, are featured by the block diagram in Fig.5. Note that the shape of the transfer functions from (8)-(9), and consequently the belt-stretch response, and furthermore the closed-loop bandwidth of the position control, can be arbitrarily chosen by the control gains.

The control law can be derived following the SMC procedure described in *Section* III.A. One can find the derivative of the switchng function (5) as follows in (12).

$$\dot{\sigma} = \left(\dot{a}^c - \dddot{x}\right) - \gamma\left(\ddot{w} + \alpha \dot{w}\right) \tag{12}$$

From the first equation in (3) one can express $\ddot{w}$ (13),

$$\ddot{w} = -\omega_0^2 w + \frac{\tau - \tau_{wf}}{J} \tag{13}$$

and insert $d\ddot{w}/dt$ into (12). It yields equation (14).

$$\dot{\sigma} = \left(\dot{a}^c - \dddot{x}\right) - \gamma\left(\alpha \ddot{w} - \omega_0^2 \dot{w} + \frac{\dot{\tau} - \dot{\tau}_{wf}}{J}\right) \tag{14}$$

From condition $\dot{\sigma}(\dot{\tau} = \dot{\tau}_{eq}) = 0$ one can find the equivalent control:

$$\begin{aligned} \tau_{eq} &= \int_0^t \dot{\tau}_{eq} d\upsilon \\ \tau_{eq} &= \frac{\beta}{\omega_0^2}(J + M)\left(a^c - \ddot{x}\right) - J\left(\alpha \dot{w} - \omega_0^2 w\right) + \tau_{wf} \end{aligned} \tag{15}$$

and the σ velocity can be now expressed by (16).

$$\dot{\sigma} = -\frac{\omega_0^2}{\beta}\frac{\dot{\tau} - \dot{\tau}_{eq}}{J + M} \tag{16}$$

Here, it can be assumed that at $t = 0$ the system is relaxed, i.e. $\tau_{eq}(0) = 0$. From (15) one can note that the acceleration signal $\ddot{x}$ is required for the computation of the equivalent control signal τ_{eq}. However, the use of an acceleration signal should be avoided in practice where only position and/or velocity sensing devices are available. Therefore, $\ddot{x}$ will be replaced in the formulation of τ_{eq}. From (3), the second equation, one can express $\ddot{x}$:

$$\ddot{x} = \frac{Kw - f_f}{M} \tag{17}$$

and insert it into (15). The equation of the equivalent control signal is now expressed by

$$\tau_{eq} = \frac{\beta}{\omega_0^2}(J + M)a^c - J\left(\alpha\dot{w} + (\beta - \omega_0^2)w\right) + \tau^{dist} \tag{18}$$

$$\tau^{dist} = \tau_f + \zeta f_f \tag{19}$$

where $\zeta = \kappa(\frac{\beta}{\omega_0^2} - 1) + \frac{\beta}{\omega_0^2}$, and τ^{dist} stands for the system disturbance signal. The parameter ζ is related both to the plant model parameters and the parameters of the enforced belt-stretch dynamics: if $\beta = \omega_0^2$ then $\zeta = 1$ and τ^{dist} reduces to the sum of total friction present in the uncontrolled system: $\tau^{dist} = \tau_f + f_f$.

Further derivation of the control law applies condition $\dot{\sigma} = -D\sigma$ in order to obtain continuous control signal τ. Application of the equivalent control method yields control that explicitly involves τ_{eq} along with τ^{dist} that is not a measurable signal in real applications. Hence, the equivalent control signal τ_{eq} is replaced with its estimated value $\hat{\tau}_{eq}$,

$$\hat{\tau}_{eq} = \frac{\beta}{\omega_0^2}(J + M)a^c - J\left(\alpha\dot{w} + (\beta - \omega_0^2)w\right) \tag{20}$$

and the control signal τ is given by (21),

$$\tau = \int_0^t \dot{\tau} d\upsilon = \hat{\tau}_{eq} + \int_0^t \dot{\tau}_{SMC} d\upsilon \tag{21}$$

where

$$\dot{\tau}_{SMC} = \frac{\beta}{\omega_0^2}(J+M)D\sigma\,. \tag{22}$$

The control law (21) has two components. One is representing estimation of the equivalent control. Another can be referred to as robust controller that is representing the disturbance estimation and the convergence to the selected sliding mode manifold. With the insertion of the control algorithm (20)-(22) into (16) one can yield the system motion projection on the σ-space that is governed by (23),

$$\dot{\sigma} + D\sigma = \frac{\omega_0^2}{\beta}\frac{\dot{\tau}^{dist}}{J+M} \tag{23}$$

which gives for $D > 0$ asymptotically stable reaching phase: convergence to steady state is dictated by the value of the right hand side in (23). In order to have stable solution $\sigma = 0$ the disturbance should satisfy the requirement $\dot{\tau}^{dist} = 0$, or in other words, it should be constant. If disturbance changes slowly ($\dot{\tau}^{dist} \approx 0$), the control law keeps the system states in the vicinity of the sliding mode manifold ($\sigma \approx 0$).

An important characteristic of a closed-loop system is also a relation, which describes influence of disturbance signal on system state variables. In this paper, such relation between the system state σ and the disturbance signal τ^{dist} is determined by the disturbance sensitivity function $F_{dist}(p)$.The disturbance sensitivity transfer function can be derived from (23) in the form described by (24),

$$F_{dist}(p) = \frac{p}{p+D} \tag{24}$$

i.e. high-pass filter of first order, which guarantees elimination of steady state error. More details about the control law defined by (20)-(22) can be found in [20]. The authors have also shown that acceleration is not required for calculation of the control signal τ though involved in the switching function (5). Thus noise problems related to the acceleration measurement are eliminated from the implementation.

C. SMC With Disturbance Observer

The estimation of the equivalent control signal (20) does not contain any information about the disturbance signal τ^{dist}. Although the closed-loop system dynamics can have asymptotic convergence to the equilibrium in steady state, it will not guarantee zero tracking error if the fast changes in the

disturbance signal exist (as it is shown by (23)). In addition, the disturbance signal in servo systems will inevitably involve friction and stiction phenomenon (dynamic and static friction) that will cause discontinuous change at the points of velocity reversals. The proposed control law (20)-(21) will not be able to compensate the friction effects instantaneously though it shows robustness against the dynamic friction. The error peaks can be minimized in amplitude as well as in time duration by selecting large D, however, in practice upper limit always exists, which depends on unmodeled dynamics, measurement noise, and finite control rate. Very high gain can cause oscillations or even unstable plant response. In [21] a combination of the disturbance observer and standard SMC scheme has been proposed to eliminate the problems with friction and fast changing disturbances.

In order to eliminate the drawbacks of the control (20)-(21) that yields closed loop motion (23), it is proposed in this paper to construct the control signal as depicted by Fig.6. In the proposed solution assume that the system dynamics can be represented by nominal plant dynamics which is perturbed by the system disturbance signal. The equivalent control $\hat{\tau}_{eq}$ that is designed by the model-based estimation approach is now combined with an additional disturbance estimation signal $\hat{\tau}^{dist}$ that may be obtained by an application of a disturbance observer scheme. The proposed control law, which is introduced by (25),

$$\tau = \left(\hat{\tau}_{eq} + \hat{\tau}^{dist}\right) + \int_0^t \dot{\tau}_{SMC} d\upsilon \tag{25}$$

has three components. The model based equivalent control estimation and the disturbance observer output signal are constituting the estimation of the equivalent control, and another is signal from the robust sliding mode controller that is now representing the mismatch in the disturbance estimation and the convergence to the selected sliding mode manifold. Thus, with the control (25) the σ-dynamics from (23) converts to (26),

$$\dot{\sigma} + D\sigma = \frac{\omega_0^2}{\beta} \frac{\Delta \dot{\tau}^{dist}}{J + M} \tag{26}$$

where $\Delta\tau^{dist}$ stands for disturbance estimation error $\Delta\tau^{dist} = \tau^{dist} - \hat{\tau}^{dist}$. It is obvious that by selecting proper convergence rate of the disturbance observer, the right hand side of the equation (26) will vanish and the robust asymptotic reaching phase will be established as it is described by (27).

$$\dot{\sigma} + D\sigma = 0 \tag{27}$$

D. Construction of The System Disturbance Observer

The disturbance observer paradigm [6] has attracted lots of attention among the motion control research community. It has been also successfully applied in the torsional elastic servosystems where the motor shaft is affected by reaction torque as well. The disturbance rejection framework in conjunction with "resonance ratio controller" [8][9] can be used in the stabilization and control of systems with elastic links.

The asymptotic disturbance observer [6] has a well known structure in motion control. Its application, as depicted in Fig.7-a, satisfies the dynamics described by (28), if estimated reaction torque $\hat{\tau}^{reac}$ matches the actual value of τ^{reac}.

$$\dot{\hat{\tau}}^{dist} + g\hat{\tau}^{dist} = g\tau^{dist} \tag{28}$$

It can estimate the motor side disturbance but cannot estimate the system disturbance τ^{dist} which is given by (19). It appears in our closed-loop system described by (3), (20), (21), and is a combination of friction as well as plant and control parameters. In order to determine it not only motor side friction but also the load side friction should be estimated. One solution is to form the system disturbance estimation signal $\hat{\tau}^{dist}$ as given by (29).

$$\hat{\tau}^{dist} = \hat{\tau}_f + \zeta\hat{f}_f \tag{29}$$

In the design of motor side disturbance observer, one can consider that driving torque (or motor current) and velocity are measurable signals. In order to properly estimate friction on the motor side, the observer must be compensated for the reaction torque (see (2)) that is not a measurable signal, but from stretch measurement it can be estimated by (30).

$$\hat{\tau}^{reac} = L\hat{f}^{reac}, \ \hat{f}^{reac} = \hat{K}w \tag{30}$$

Having available belt-stretch signal, then the motor friction can be estimated by the disturbance observer depicted by Fig.7-a. Its output is constructed as described by (31).

$$\hat{\tau}_f = \frac{g}{p+g}\left((\tau - \hat{\tau}^{reac}) - J\ddot{\varphi}\right) \tag{31}$$

The similar disturbance observer can be applied for estimation of the load-side friction. The belt-stretch and the position (and the velocity) of the carriage are assumed to be available signals. The load-side driving force is the reaction force due to the stretch of the belt. Hence, it can be estimated as in (30). The structure of the proposed load-side disturbance observer is depicted in Fig.7-b. The observer output is given by equation (32).

$$\hat{f}_f = \frac{g}{p+g}\left(\hat{f}^{reac} - M\ddot{x}\right) \tag{32}$$

Finally, the estimated system disturbance signal $\hat{\tau}^{dist}$ is synthesized as described by (29). The block diagram of the proposed system disturbance observer structure is shown in Fig.7-c.

E. Closed-loop analysis

After short algebra by combination of (2) and (29)-(32) one can yield the equation of the system disturbance observer output signal (33),

$$\hat{\tau}^{dist} = \frac{g}{p+g}\left(\tau_f + \zeta f_f + (1-\zeta)\Delta\tau^{reac}\right) = \frac{g}{p+g}\left(\tau^{dist} + (1-\zeta)\Delta\tau^{reac}\right) \tag{33}$$

where $\Delta\tau^{reac} = \tau^{reac} - \hat{\tau}^{reac}$. Obviously, the proposed observer will estimate the required system disturbance signal with the prescribed first order dynamics. The disturbance observer estimation delay can be tuned arbitrarily by the observer gain g. The disturbance estimation error of the proposed observer can be expressed by (34)

$$\Delta\tau^{dist} = \frac{p}{p+g}\tau^{dist} - \frac{g}{p+g}(1-\zeta)\Delta\tau^{reac} \tag{34}$$

and thus (26) can be rewritten as shown by (35).

$$\dot{\sigma} + D\sigma = \frac{\omega_0^2}{\beta}\frac{\frac{p}{p+g}\dot{\tau}^{dist} - \frac{g}{p+g}\Delta\dot{\tau}^{reac}}{J+M} \tag{35}$$

To analyze the closed-loop behavior, firstly, let assume ideal reaction force estimation ($\Delta\tau^{reac} = 0$). Then, the disturbance estimation error reduces as in (36).

$$\Delta\tau^{dist} = \frac{p}{p+g}\tau^{dist} \tag{36}$$

The closed-loop dynamics are now described by equations (36), (26), and (7), that is the disturbance estimation error dynamics, the dynamics equation of the convergence to the sliding manifold, and finally, the dynamics of the system output, respectively. One can rewrite the disturbance sensitivity function from (24) considering the proposed control law with the disturbance observer. It can be derived from (26) and (36).

$$F_{dist}(p) = \frac{p^2}{(p+D)(p+g)} \tag{37}$$

The disturbance sensitivity function can be now described as a second order high-pass filter, which suppresses disturbance in low-pass frequency domain. By application of the proposed disturbance observer the order of disturbance suppression rate is now increased by one in comparison with (24). Typically, (37) suggests to tune both gains D and g as large as possible in order to increase cut-off frequency and to achieve good disturbance rejection.

However, a portion of the reaction torque will be present in the signal if the mismatch between the real and estimated value of the reaction torque exists. The velocity of the reaction torque mismatch signal $\Delta\tau^{reac}$ appears on the right-hand side of the σ-dynamics equation. The influence of $\Delta\tau^{reac}$ on the system state σ can be determined by the reaction torque mismatch sensitivity transfer function $F_{reac}(p)$ derived from (35). $F_{reac}(p)$ can be given by (38).

$$F_{reac}(p) = \frac{p}{p+D}\frac{g}{p+g} \tag{38}$$

Obviously, it is important to ensure the reaction torque compensation as good as possible since it has a large impact on the disturbance estimation accuracy. If one can rely on the reaction force estimation signal, the disturbance output will follow the real friction value with the prescribed dynamics as required by the

equation (28). However, in practice this is hardly possible due to the parameters variation and model uncertainties. Accuracy of the disturbance estimation signal will affect the control performance though every mismatch between the real disturbance signal and the observer output will be compensated by the SMC part of the proposed control law. However, it can be shown, that the presence of the reaction torque in the observed disturbance signal, creates an additional virtual loop in the closed-loop system (as shown by (35) and (38) σ and $\Delta\tau^{reac}$ are related by $F_{reac}(p)$, but on the other hand $\Delta\tau^{reac}$ is again related to σ by $H_w(p)$, i.e. $\Delta\tau^{reac}$ is obviously directly connected to w, and w is in turn linked to σ by $H_w(p)$, as follows from (6) and (10)). Stability of this virtual loop can not be always guaranteed. Thus it can destabilize the closed-loop system or allow for poor performance only. Hence, $F_{reac}(p)$ should be also considered in the design the disturbance observer filter. The sensitivity transfer function $F_{reac}(p)$ can be described as a second order filter with two first-order filters in series: the first portion is related to the robust SMC design and contributes a high-pass filter whereas the second portion is the disturbance observer filter that contributes a low-pass filter. $F_{reac}(p)$ should be designed to suppress the reaction torque mismatch signal as much as possible in the entire frequency domain. This implies that the cut-off frequencies of the low-pass filter and high-pass filter should be wide apart. Hence, the trade-off between the speed of the disturbance observation and system stability will dictate the disturbance observer design.

IV. Experimental Results

The experiments were carried out on a low-cost linear timing-belt servomechanism. A DC-motor was attached to the linear belt-drive via a gearbox with speed reduction ratio G=29, and the pulley diameter of 12cm. The traveling path of the carriage was about 2m. The motor angle was measured by optical incremental encoder which assured 5000 p/rev, whereas the carriage position was measured by a magnetic tape that enabled measurement resolution of 0.01 mm. The diagram of the control system used in the experiments is shown by Fig.8. Typical characteristic of the linear belt drive is depicted by Fig.9 (though it varies over the traveling path). The drive features high friction and backlash that can be observed in the

belt-stretch response. Tables I, II give the parameters of the experimental system used in the experiments. The model parameters M_m and M_l stand for the reflected mass of motor inertia and the load mass (carriage), respectively. ω_0 is the first resonance frequency of the drive-train, that was determined on the basis of frequency analysis of the belt-stretch signal shown by Fig.9-b. K is estimated value of the belt-stiffness coefficient that was calculated by the following equation

$$K = \omega_0^2 / \left(\frac{1}{M_m} + \frac{1}{M_l} \right)$$

that can be derived from (4). The controller gains are actually parameters of the prescribed closed-loop dynamics that is best it could be achieved. The controller was executed with the sampling period of 2ms.

The experimental results are shown in Fig.10. Firstly, the disturbance estimation performance was tested by comparison between the control by the pure SMC algorithm (21) and the control with the proposed observer (25) at D=0, i.e. the disturbance estimation by SMC was off. In the first case, the system disturbance observer was also implemented, but not connected in the loop. The results are shown by Fig.10-a and Fig.10-b, respectively. In Fig.10-a the disturbance estimation signals are practically overlapped. However, the observer dynamics was actually slower though g=D=75. Consequently, higher position error peaks appeared as shown in Fig.10-b (here g=75, D=0). The position error peaks appeared at the points of velocity reversals due to nonlinear friction effect. These results show that the pure SMC algorithm performs better then control with the proposed disturbance observer.

Fig.10-c and Fig.10-d show results obtained by the proposed SMC with observer (25). Here, D=75 and the observer dynamics was set with g=10 and g=20 in Fig.10-c and Fig.10-d, respectively. Both, the disturbance estimation by SMC and the proposed observer with slower dynamics were connected in the control loop. As could be expected, the SMC estimated only the difference $\Delta\tau^{dist}$, i.e. the portion which the observer failed to output. It converged to zero value after the transient period. In comparison with the results shown in Fig.10-a, position error peaks are lowered in both cases. Faster dynamics of the observer caused lower position error, however, as noted by the theoretical analysis in *Section* III.E, only a conservative disturbance observer dynamics could be set up in order to preserve stability of the system.

Larger values of the observer gain g caused oscillations in the system and ultimately led to instability. Thus, the disturbance observer cut-off frequency was rather limited in the experiments.

Finally, experimental results at high reference speed are also presented. The results obtained by the pure SMC algorithm are shown in Fig. 10-e (the disturbance observer is implemented but not connected in the loop as in Fig.10-a), whereas Fig.10-f includes the results obtained by the proposed SMC with observer at g=20. The diagrams show that the proposed control scheme extended by the system disturbance observer lower position error peaks in amplitude and time duration both at low-speed and high speed experiments.

V. CONCLUSION

The paper has proposed a new SMC control algorithm that is extended with the asymptotic disturbance observer in order to improve position tracking performance at the points of velocity reversals, where error peaks appear due to nonlinear friction characteristic. The disturbance observer has been designed to estimate the system disturbance signal identified by the equivalent control that is not measurable. It requires the reaction force signal for the realization, which is often not available in practice. Thus, it should be estimated as proposed in this paper. It has been shown, that the compensation of the reaction force is of significant importance for accuracy of the disturbance estimation, stability and performance improvement of the closed-loop system. The estimated disturbance signal, which is perturbed by the reaction force, can destabilize the system or only slow disturbance estimation dynamics can be achieved. However, the experimental results have shown that even in the case of the erroneous model used in the determination of the reaction force signal, improvement in the position error response has been evident. The proposed scheme lower position error peaks in amplitude and time duration both at low-speed and high speed experiments.

VI. ACKNOWLEDGEMENT

The authors gratefully acknowledge the contributions of ARRS-Slovenian Research Agency, and Tübitak, The Scientific and Technical Research Council of Turkey, which partly financially supported the joint research project "Sliding Modes in Motion Control Systems" of Institute of Robotics, University Of Maribor, and Faculty of Engineering and Natural Science, Sabanci University, Istanbul-Turkey.

REFERENCES

[1] M. Kagotani, T.Koyama, H. Ueda, "A study on transmission error in timing belt drives," *ASME Journal of Mechanical Design*, Vol. 115, No. 12, pp. 1038-1043, 1993.

[2] S. Abrate, "Vibration of belts and belt-drives," *Mechanism and machine theory*, Vol. 27, No. 11, pp. 645-659, 1992.

[3] Y. Hori, "Vibration suppression and disturbance rejection control on torsional systems," in *Proc. of IFAC Workshop on Motion Control*, 1995, Munich, Germany , pp. 41-50.

[4] I. Godler, M. Inoue, T. Ninomiya, T. Yamashita, "Robustness comparison of control schemes with disturbance observers and with acceleration control loop," in *Proc. of IEEE ISIE*, 1999, Bled, Slovenia, pp.1035-1040.

[5] P.B. Schmidt, R.D. Lorenz, "Design principles and implementation of acceleration feedback to improve performance of DC drives," *IEEE Trans. on Industry Applications*, Vol. 28, No. 3, pp. 594-599, 1992.

[6] K. Ohnishi, M. Shibata, T. Murakami, "Motion control for advanced mechatronics," *IEEE/ASME Trans. on Mechatronics*, Vol. 1, No. 1, pp. 56-67, 1996.

[7] H. Kawaharada, I. Godler, T. Ninomiya, H. Honda, "Vibration suppression control in 2-inertia system by using estimated torsion torque," in *Proc. of IEEE IECON*, 2000, Nagoya-Japan, pp. 2219-2224.

[8] K. Yuki, T. Murakami, K. Ohnishi, "Vibration control of 2 mass resonant system by resonance ratio control," in *Proc. of IEEE IECON*, 1993, Vol. 3, pp. 2009-2014.

[9] Y. Hori, H. Sawada, Y. Chun, "Slow resonance ratio control for vibration suppression and disturbance rejection in torsional system," *IEEE Trans. on Industrial Electronics*, Vol. 46, No. 1, pp. 162-168, 1999.

[10] M. Matsuoka, T. Murakami, K. Ohnishi, "Vibration Suppression and Disturbance Rejection Control of Flexible Link Arm", in *Proc. of the IECON*, 1995, Vol. 2, pp. 1260-1265.

[11] S. Katsura, J. Suzuki, K. Ohnishi, "Pushing Operation by Flexible Manipulator Taking Environmental Information into Account," in *Proc. of the AMC*, 2004, Kawasaki, Japan, pp. 141-146.

[12] R. Gorez, Y-L. Hsu, "Sliding mode control for displacements of servomechanisms with elastic joints," in *Proc. of the 13th IFAC Triennial World Congress*, 1996, San Francisco-USA, pp.43-48.

[13] P. Korondi, H. Hashimoto, V. Utkin, "Direct torsion control of flexible shaft in an observer-based discrete-time sliding mode," *IEEE Trans. on Industrial Electronics*, 1998, Vol. 45, No. 2, pp.291-296.

[14] Y-F. Li, B. Eriksson, J. Wikander, "Sliding mode control of two-mass positioning systems," in *Proc. of the 14th IFAC Triennial World Congress*, 1999, Beijing-China, pp.151-156.

[15] V.I. Utkin, *Sliding Modes in Control and Optimization*. Springer-Verlag, Berlin, 1992.

[16] A. Šabanović, K. Jezernik, K. Wada, "Chattering-free sliding modes in robotic manipulators control," *Robotica*, Vol.17, No. 29., pp.17-29, 1996.

[17] A. Hace, K. Jezernik, M. Terbuc, "Robust accurate motion control for belt-driven servomechanism," in *Recent Advances In Mechatronics*, Kaynak, O., Editor. Springer-Verlag, Singapore, 1999.

[18] A. Šabanović, Y. Yildiz, K. Abidi, N. Šabanović, "Sliding Mode Control of Timing-Belt Servo-system," in *Proc. of EDPE*, 2003, The High Tatras, Slovak Republic, pp.55-60.

[19] A. Hace, K. Jezernik, M. Terbuc, "VSS motion control for a laser cutting machine," *Control Engineering Practice*, Vol. 9, No. 1, pp. 67-77, 2001.

[20] A. Hace, K. Jezernik, A. Šabanović, "Improved Design of VSS Controller for a Linear Belt-Driven Servomechanism," *IEEE/ASME Transactions on Mechatronics*, Vol. 10, No. 4, pp. 385-390, August 2005.

[21] Y. Fujimoto, A. Kawamura, "Robust servo-system based on two-degree-of-freedom control with sliding mode," *IEEE Transactions on Industrial Electronics*, Vol. 42, Issue 3, pp. 272 – 280, June 1995.

[22] A. Šabanović, "Sliding Mode Framework in Motion Control. What it Offers?," in *Proc. of AMC*, 2004 March 25-28, Kawasaki, Japan, pp.1-10.

[23] B. Draženović, "The invariance conditions in variable structure systems," *Automatica*, Vol. 5, pp. 287-295, 1969.

LIST OF FIGURES

LIST OF TABLES

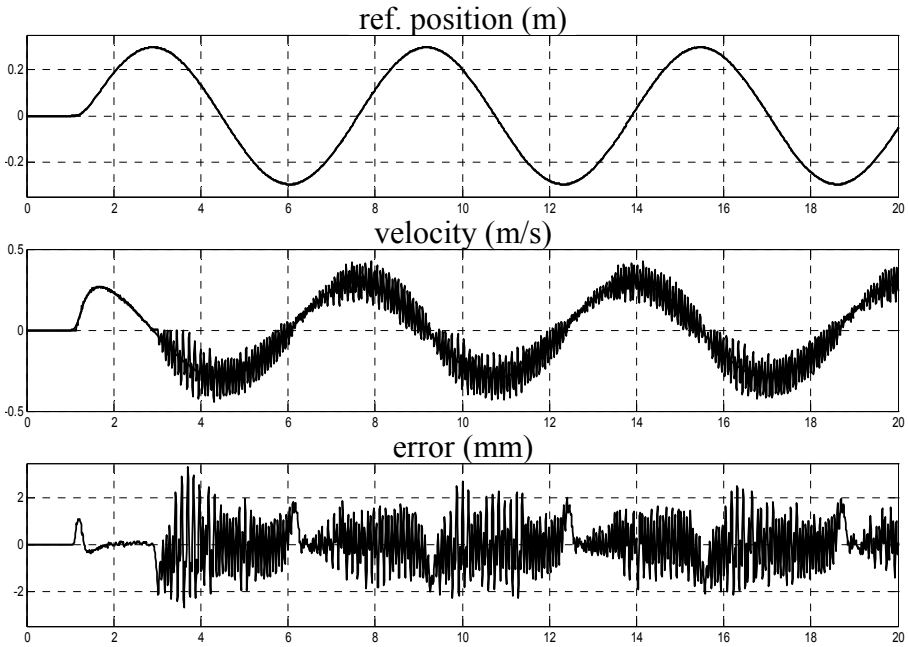

Figure 1. Vibrated response of a linear belt-drive

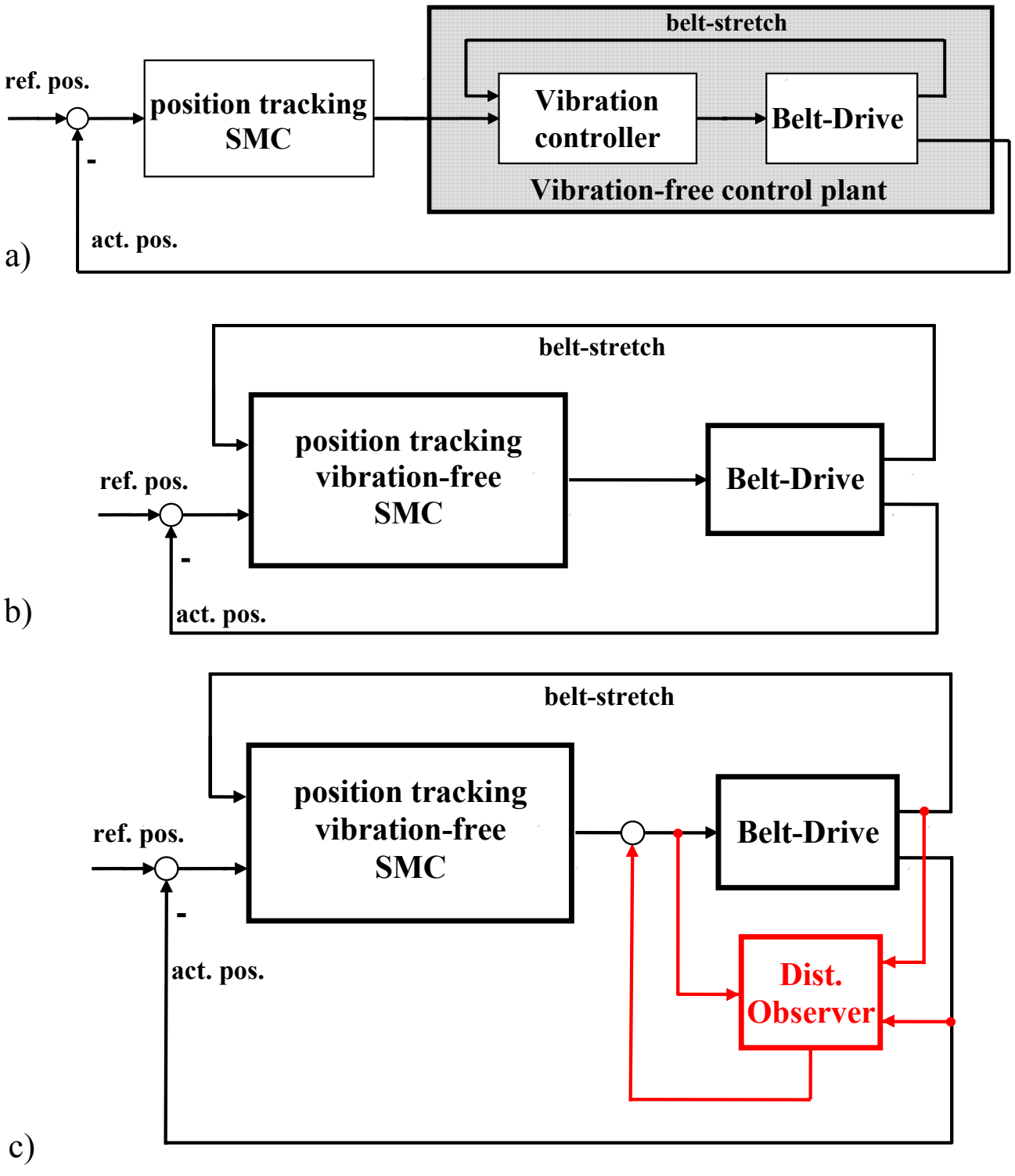

Figure 2. Different control structures of a linear belt-drive:
a) Cascaded control structure, b) Single loop control structure, c) SMC with disturbance observer

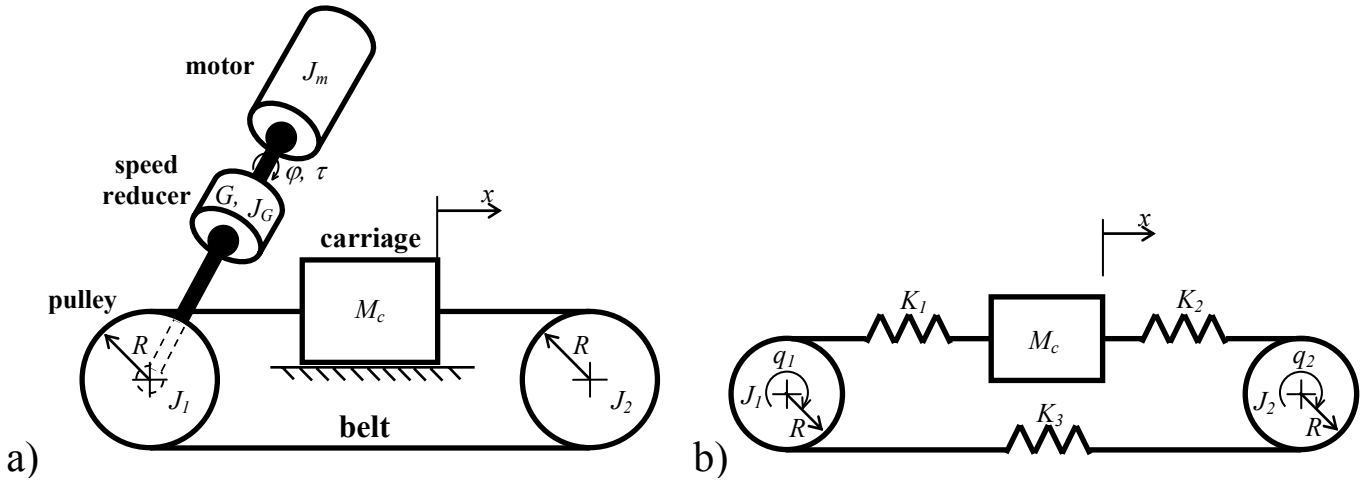

Figure 3. Linear belt-drive: a) Servomechanism, b) Spring model of the belt drive

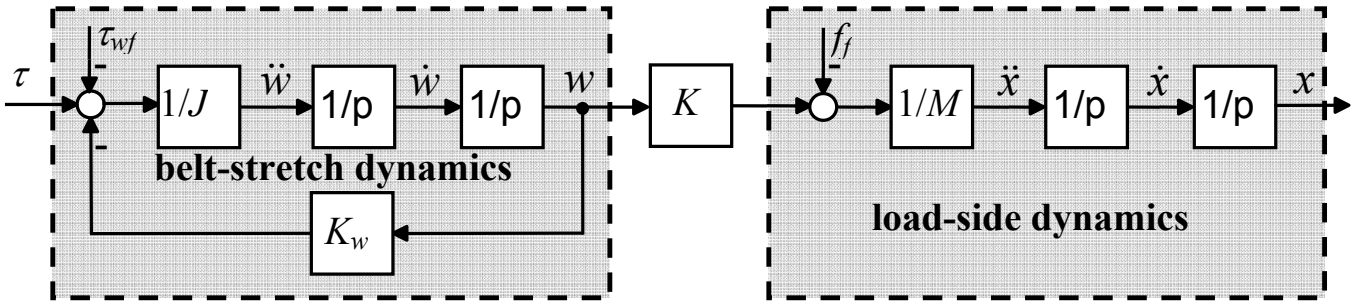

Figure 4. Block diagram of the belt-stretch model

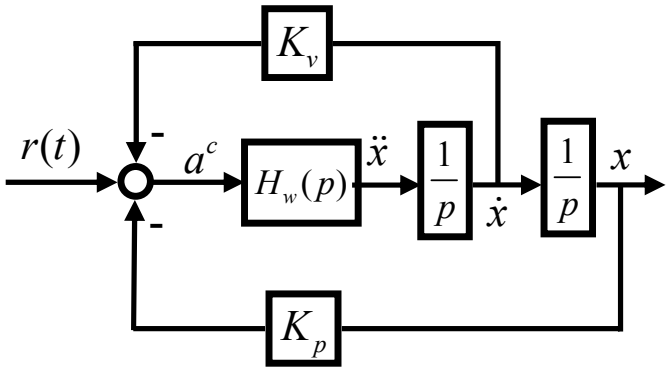

Figure 5. Closed-loop block diagram in sliding mode

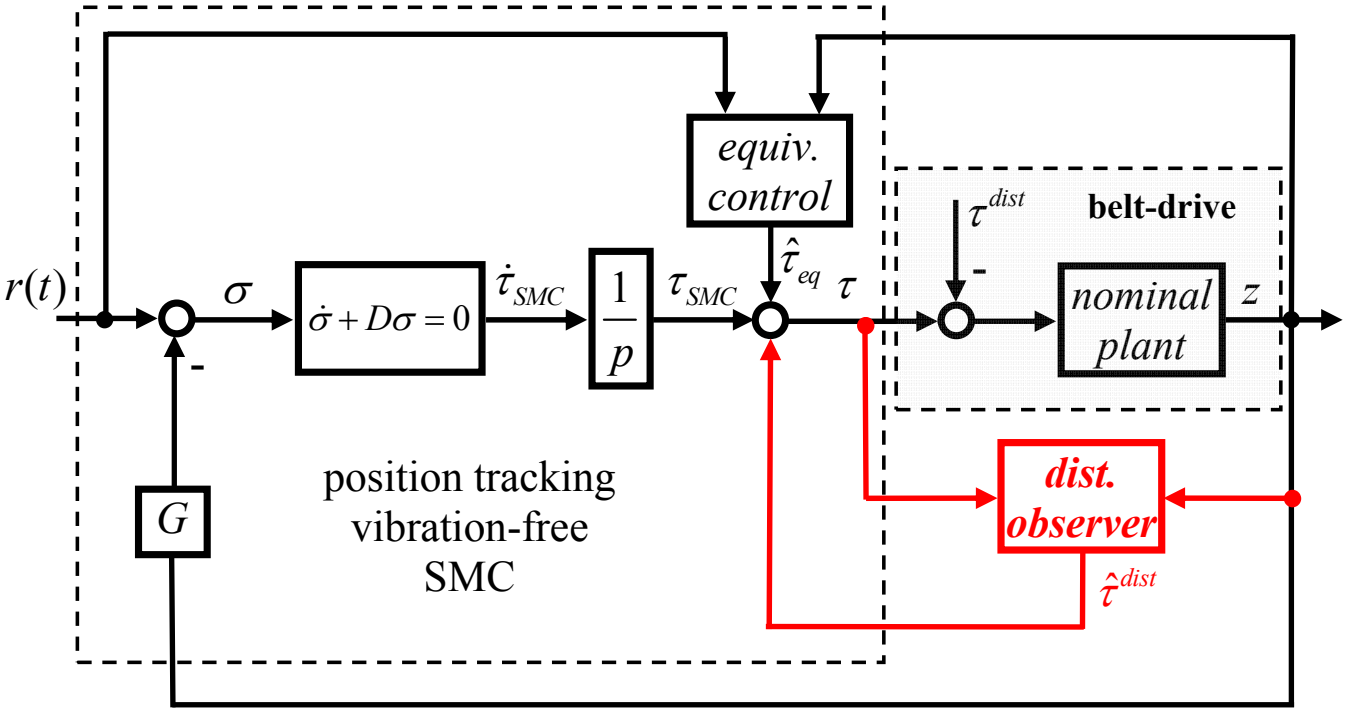

Figure 6. Chattering-free SMC with disturbance observer

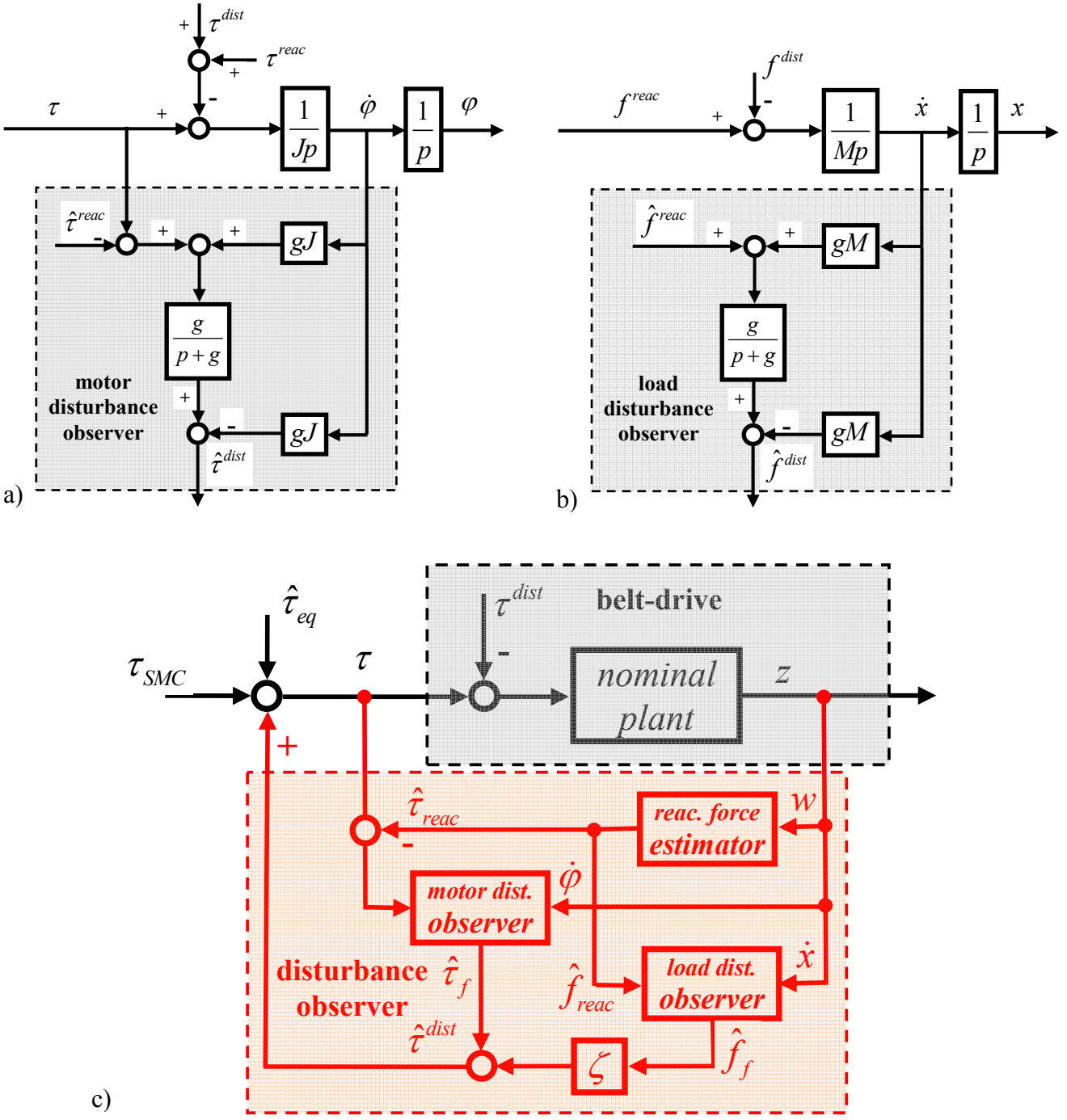

Figure 7. Proposed disturbance observer structure: a) Motor disturbance observer, b) Load disturbance observer, c) System disturbance observer

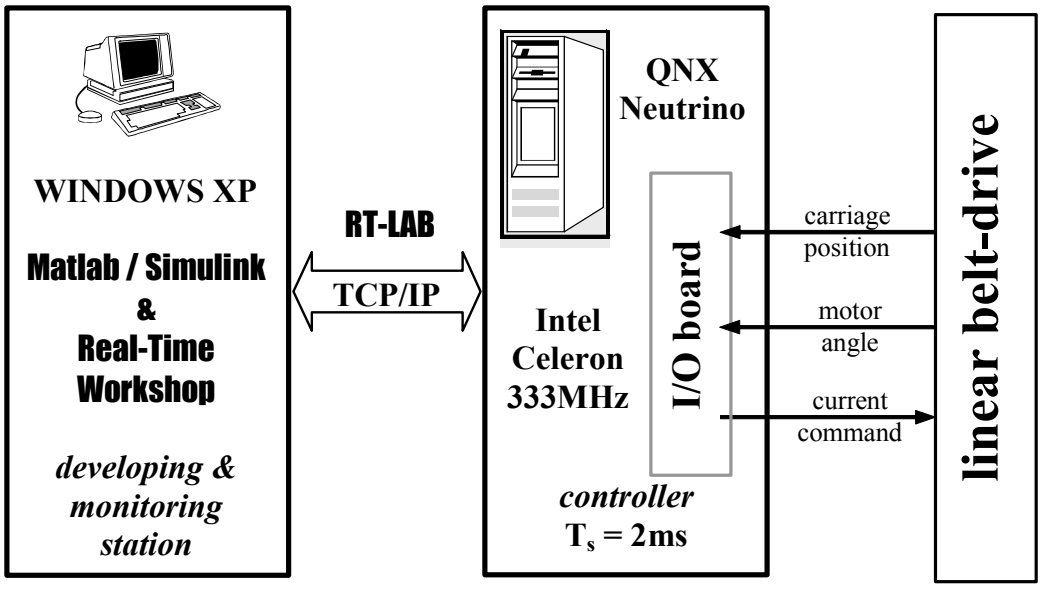

Figure 8. Experimental control system

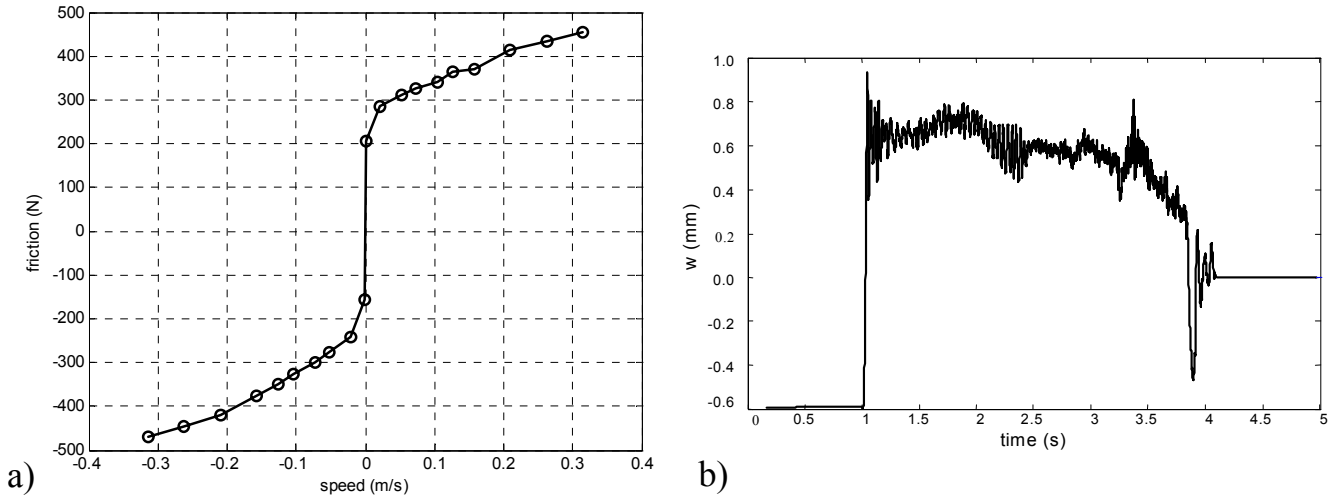

Figure 9. Typical response of the experimental linear drive: a) friction characterics, b) open-loop belt-stretch response

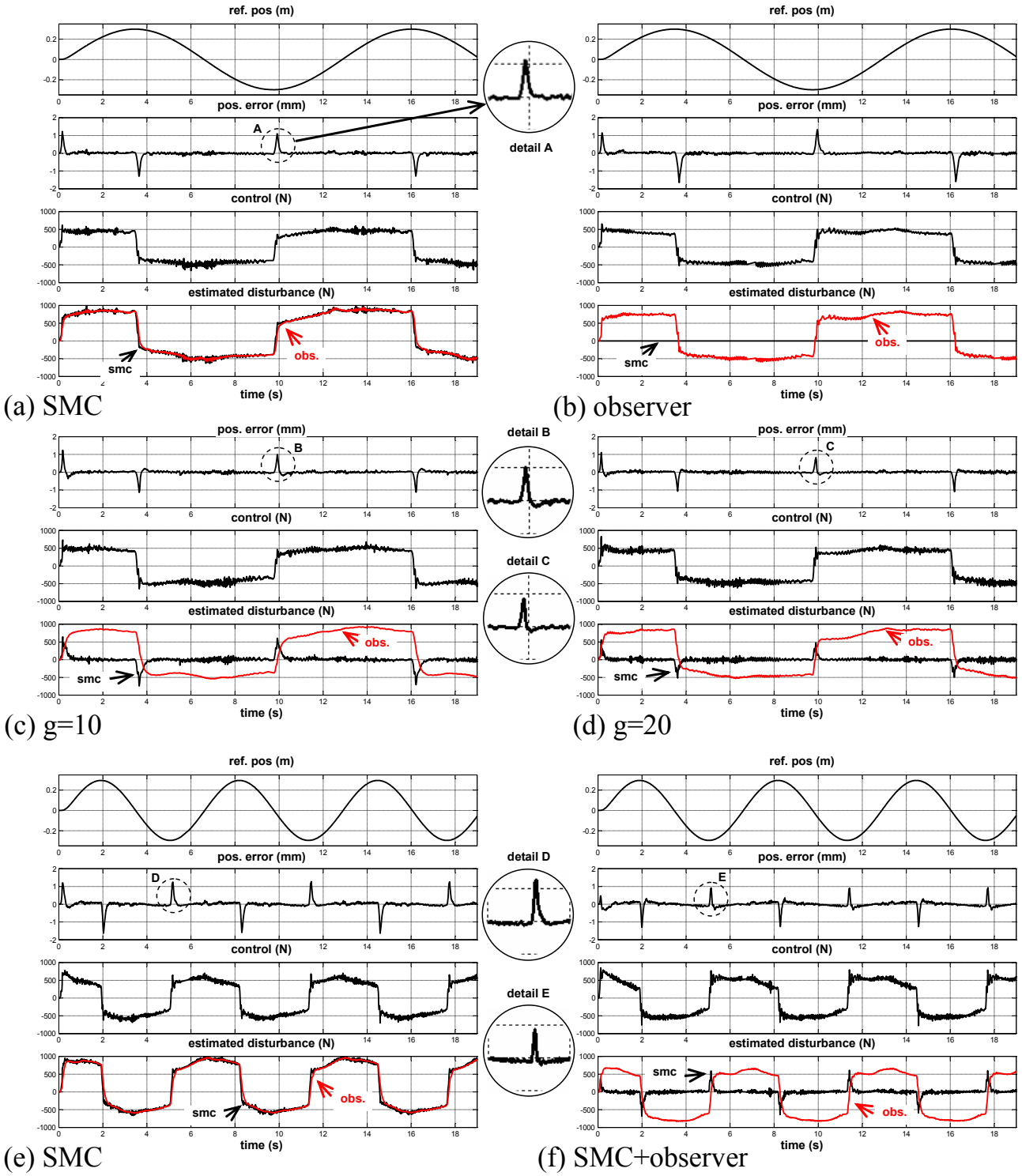

Figure 10. Experimental results:
a) SMC without dist. observer; b) control with dist. observer at D=0 and g =75; SMC with dist. observer at c) g=10, and d) g=20; test at high speed e) SMC without dist. observer, and f) SMC with dist. observer

TABLE I.
MODEL PARAMETERS

M_m	M_l	ω_0	K
(kg)	(kg)	(rad/s)	(N/m)
57	33	62.8	2.7e5

TABLE II.
CONTROLLER GAINS

D	α	β	K_v	K_p
75	125.6	7888	50	625